

Stieltjes-integral approximations to photoabsorption and dispersion profiles in atomic helium*

P. W. Langhoff, J. Sims, and C. T. Corcoran

Department of Chemistry, Indiana University, Bloomington, Indiana 47401

(Received 15 May 1974)

Variational calculations in Hilbert space and theorems from the theory of moments are employed in the construction of Stieltjes-integral approximations to the electric-dipole absorption and dispersion profiles in atomic helium. A spectrum of discrete transition frequencies and oscillator strengths obtained from variationally determined pseudostates furnishes accurate approximations to the necessary dipole spectral sums. Solution of the appropriate moment equations, or transformation to a basis set of principal pseudostates, provides the principal frequencies and strengths necessary for Stieltjes imaging the absorption profile, and for the evaluation of the associated dispersion profile. Rapid convergence is obtained to values in excellent agreement with the available experimental absorption cross section, refractive index, and Verdet coefficient, and with semiempirical estimates of the closely related dynamic dipole shielding factor and Rayleigh-scattering cross section. Moreover, comparison of the discrete pseudospectrum of frequencies and strengths with its Stieltjes average indicates the presence of approximations to autoionizing states and inelastic thresholds in the variationally determined photoabsorption profile. These results suggest that the Stieltjes technique for determining photoabsorption and dispersion profiles is a useful complement to more conventional methods which require the explicit construction of discrete and continuum eigenfunctions.

I. INTRODUCTION

Schrödinger dynamics provides a formal basis for investigating the resonant absorption¹ and non-resonant dispersion² of electromagnetic radiation in matter. The expressions obtained in the semiclassical approximation for absorption and dispersion cross sections,³ however, generally require construction of the appropriate complete set of discrete and continuum target eigenfunctions.⁴ Consequently, attention has been devoted to the formulation of alternative techniques which are more appropriate for computational applications.⁵ A recently described Stieltjes-imaging technique avoids explicit construction of discrete and continuum eigenfunctions, and can provide accurate approximations to both photoabsorption and dispersion profiles.⁶

In the present paper, the Stieltjes technique is employed in a detailed *ab initio* calculation of the photoabsorption and dispersion profiles in atomic helium. Standard Ritz variational calculations and large basis sets are used to construct an accurate 1S_0 ground-state eigenfunction and a 1P_1 spectrum of square-integrable pseudostates. The latter provide discrete transition frequencies and oscillator strengths and associated spectral moments,⁷ from which the correct oscillator-strength distribution is derived employing the Stieltjes-imaging technique. The necessary principal transition frequencies and oscillator strengths are obtained from

solutions of the appropriate moment equations,⁸ or, alternatively, from a transformation of the original pseudospectrum to a basis set of principal pseudostates.⁶ It is found that the Stieltjes procedure is rapidly convergent in the case of atomic helium, and that relatively small numbers of spectral moments (~10) or principal pseudostates (~5) give highly accurate approximations to the photoabsorption cross section and refractive index, and to the closely related dynamic dipole shielding factor, Verdet coefficient, and Rayleigh-scattering cross section. Moreover, comparison of the variationally calculated oscillator-strength distribution and its associated Stieltjes average suggests the presence of autoionizing line shapes and inelastic thresholds at the appropriate frequencies.⁹

The photoabsorption and dispersion profiles are defined in Sec. II, variational calculations described in Sec. III, Stieltjes imaging discussed in Sec. IV, and the numerical results presented in Sec. V. Some concluding remarks are made in Sec. VI.

II. PHOTOABSORPTION AND DISPERSION PROFILES

The photoabsorption index and associated refractive index of a dilute atomic gas can be written in the forms^{10,11}

$$k(\omega) = (4\pi N_0/c)\omega \operatorname{Im} \alpha(\omega), \quad (1a)$$

$$n(\omega) - 1 = 2\pi N_0 \operatorname{Re} \alpha(\omega), \quad (1b)$$

respectively, where ω is the applied frequency, c the speed of light *in vacuo*, N_0 the number of gaseous atoms per unit volume, and

$$\alpha(z) = \int_0^\infty df(\epsilon) / (\epsilon^2 - z^2) \quad (2)$$

is the complex-valued dynamic dipole polarizability.¹² In Eq. (2),

$$df(\epsilon) = \left(\sum_{i=1}^\infty f_i \delta(\epsilon_i - \epsilon) + g(\epsilon) \right) d\epsilon \quad (3)$$

is the oscillator strength for transition into the frequency interval ϵ to $\epsilon + d\epsilon$, with f_i and $g(\epsilon)$ the discrete and continuum oscillator strengths and density,⁴ respectively, the ϵ_i are discrete transition frequencies, where $\epsilon_\infty = \epsilon_i$ is the first threshold for photoionization, and the Dirac δ functions have their customary meaning. The nondecreasing cumulative oscillator-strength distribution

$$f(0) = 0, \quad (4)$$

$$f(\epsilon) = \int_0^\epsilon df(\epsilon')$$

has an infinite number of discontinuous points of increase (f_i) at the ϵ_i values, is generally smooth in the interval $\epsilon_i \leq \epsilon < \infty$, and has structure in the neighborhood of autoionizing states and inelastic thresholds.¹

The polarizability of Eq. (2) also determines the closely related dynamic dipole shielding factor¹³

$$\gamma(\omega) = N + \omega^2 \operatorname{Re} \alpha(\omega), \quad (5)$$

the Rayleigh-scattering cross section¹⁴

$$\sigma(\omega) = (24\pi/9)(\omega/c)^4 \operatorname{Re} \alpha(\omega)^2, \quad (6)$$

and the Verdet coefficient¹⁵

$$V(\omega) = (1/2c^2)\omega dn(\omega)/d\omega, \quad (7)$$

where N is the number of atomic electrons. In addition, other dipole properties can be determined from the polarizability of Eq. (2) or from the distribution of Eq. (3), including two- and three-body dispersion forces¹⁶ and mean energies appropriate for the penetration of fast-charged particles in matter.^{1,17}

III. VARIATIONAL CALCULATIONS

Bounds on the positive- and negative-frequency components of the polarizability

$$\alpha_\pm(\omega) = \int_0^\infty df(\epsilon) / 2\epsilon(\epsilon \pm \omega) \quad (8)$$

are obtained from the functionals¹⁸

$$\begin{aligned} \mathcal{J}[\tilde{\phi}_\pm^{(1)}] = & \langle \tilde{\phi}_\pm^{(1)} | H^{(0)} - E^{(0)} \pm \omega | \tilde{\phi}_\pm^{(1)} \rangle \\ & + \langle \tilde{\phi}_\pm^{(1)} | \mu | \phi_0 \rangle + \langle \phi_0 | \mu | \tilde{\phi}_\pm^{(1)} \rangle, \end{aligned} \quad (9)$$

where $H^{(0)}$, $E^{(0)}$, and ϕ_0 are the atomic Hamiltonian and ground-state energy and eigenfunction, respectively, and μ is the dipole-moment operator in the polarization direction. Convenient trial functions are given by the linear combinations¹⁹

$$\tilde{\phi}_\pm^{(1)} = \sum_{i=1}^M a_i^\pm \tilde{\phi}_i, \quad (10)$$

where the $\tilde{\phi}_i$ are a basis of square-integrable pseudostates that satisfy

$$\langle \tilde{\phi}_i | H^{(0)} - E^{(0)} | \tilde{\phi}_j \rangle = \tilde{\epsilon}_i \delta_{ij}, \quad (11a)$$

$$\langle \tilde{\phi}_i | \tilde{\phi}_j \rangle = \delta_{ij}, \quad i, j = 1, 2, \dots, M, \quad (11b)$$

and are complete in the limit $M \rightarrow \infty$. Employing Eqs. (10), (11a), and (11b), the functionals of Eq. (9) at their stationary points give

$$\tilde{\alpha}_\pm(\omega) = -\mathcal{J}[\tilde{\phi}_\pm^{(1)}] = \sum_{i=1}^M \frac{\tilde{f}_i}{2\tilde{\epsilon}_i(\tilde{\epsilon}_i \pm \omega)}, \quad (12)$$

and the polarizability is given by

$$\tilde{\alpha}(\omega) = \tilde{\alpha}_+(\omega) + \tilde{\alpha}_-(\omega) = \sum_{i=1}^M \frac{\tilde{f}_i}{\tilde{\epsilon}_i^2 - \omega^2}, \quad (13a)$$

with

$$\tilde{f}_i = 2\tilde{\epsilon}_i |\langle \tilde{\phi}_i | \mu | \phi_0 \rangle|^2. \quad (13b)$$

The approximations of Eqs. (12), (13a), and (13b) give the bounds²⁰

$$\tilde{\alpha}_+(\omega) \leq \alpha_+(\omega), \quad 0 \leq \omega < \infty, \quad (14a)$$

$$\tilde{\alpha}_-(\omega) \leq \alpha_-(\omega), \quad 0 \leq \omega < \epsilon_1, \quad (14b)$$

$$\tilde{\alpha}(\omega) \leq \alpha(\omega), \quad 0 \leq \omega < \epsilon_1, \quad (14c)$$

when the correct eigenfunction ϕ_0 is employed, where ϵ_1 is the correct resonance transition frequency. Power-series expansion of Eq. (14b) gives

$$\sum_{k=0}^\infty \tilde{S}(-k-2)\omega^k \leq \sum_{k=0}^\infty S(-k-2)\omega^k, \quad 0 \leq \omega < \epsilon_1 \quad (15)$$

where

$$\tilde{S}(-k) = \sum_{i=1}^M \tilde{\epsilon}_i^{-k} \tilde{f}_i \quad (16a)$$

and

$$S(-k) = \int_0^\infty \epsilon^{-k} df(\epsilon), \quad (16b)$$

emphasizing that the spectral sums determine the

polarizability in the normal dispersion interval. Moreover, consideration of the appropriate functionals²¹ indicates that

$$\tilde{S}(-k) \leq S(-k), \quad k = 2, 4, 6, \dots, \quad (17)$$

when a sufficiently large basis set is employed.

The sums of Eqs. (16a) and (16b) are conveniently written in the alternative forms

$$\tilde{S}(-k) = 2 \langle \phi_0 | \mu | \bar{\theta}_k \rangle, \quad (18a)$$

$$S(-k) = 2 \langle \phi_0 | \mu | \theta_k \rangle, \quad k = 1, 2, \dots, \quad (18b)$$

where

$$\bar{\theta}_k = \sum_{i=1}^M \tilde{\epsilon}_i^{(1-k)} \langle \bar{\phi}_i | \mu | \phi_0 \rangle \bar{\phi}_i, \quad (19a)$$

$$\theta_k = (H^{(0)} - E^{(0)})^{(1-k)} \mu \phi_0, \quad k = 1, 2, \dots, \quad (19b)$$

and the case $k = 1$ has been explicitly included. From Eqs. (19a) and (19b)

$$\langle \bar{\theta}_k | \bar{\theta}_l \rangle = \frac{1}{2} \tilde{S}(1 - k - l), \quad (20a)$$

$$\langle \theta_k | \theta_l \rangle = \frac{1}{2} S(1 - k - l), \quad k, l = 1, 2, \dots, \quad (20b)$$

demonstrating that the spectral sums are determined by the norms of square-integrable functions.

The θ_k of Eq. (19b) can be determined in closed form for simple and model systems.²¹ More generally, the variational approximations $\bar{\theta}_k$ of Eq. (19a) are employed in determining bounding approximations [Eqs. (17) and (18a)] to the spectral sums. The $\bar{\theta}_k$ provide a useful contraction of the original M -term pseudospectrum [Eqs. (11a) and (11b)], and can be employed as primitive basis functions in the construction of a second spectrum of $n \ll M$ (principal) pseudostates in the form

$$\bar{\phi}_i^{(\phi)} = \sum_{j=1}^n \gamma_{ji} \bar{\theta}_j, \quad i = 1, 2, \dots, n. \quad (21)$$

The $\gamma_i = (\gamma_{i1}, \gamma_{i2}, \dots, \gamma_{in})$ are obtained from

$$[\underline{H} - \tilde{\epsilon}_i(n) \underline{S}] \cdot \gamma_i = 0, \quad (22a)$$

$$\langle \bar{\phi}_i^{(\phi)} | \bar{\phi}_j^{(\phi)} \rangle = \delta_{ij}, \quad (22b)$$

where

$$(\underline{H})_{ij} = \frac{1}{2} \tilde{S}(2 - i - j) \quad (23)$$

and

$$(\underline{S})_{ij} = \frac{1}{2} \tilde{S}(1 - i - j), \quad i, j = 1, 2, \dots, n. \quad (24)$$

The n transition frequencies $\tilde{\epsilon}_i(n)$ and oscillator strengths

$$\tilde{f}_i(n) = 2\tilde{\epsilon}_i(n) |\langle \bar{\phi}_i^{(\phi)} | \mu | \phi_0 \rangle|^2 \quad (25)$$

reproduce $2n$ of the spectral moments $\tilde{S}(-k)$ identically, as a consequence of the definition of the $\bar{\theta}_k$,²¹ and are approximations to similar values

$\epsilon_i(n)$ and $f_i(n)$ obtained from the development of Eqs. (21)–(25) employing the θ_k of Eq. (19b) and the correct sums $S(-k)$ of Eq. (16b). The $\epsilon_i(n)$, $f_i(n)$ and their approximations $\tilde{\epsilon}_i(n)$, $\tilde{f}_i(n)$ have certain useful properties discussed in Sec. IV.⁶

IV. STIELTJES IMAGING

The frequencies and strengths $(\tilde{\epsilon}_i, \tilde{f}_i, i = 1, M)$ obtained from the pseudospectrum of Eqs. (11a) and (11b) are basis-set dependent, and should perhaps be regarded as unphysical,²² whereas the associated spectral moments of Eqs. (16a) and (16b) are experimentally observable, under appropriate conditions.^{23,24} Moreover, the latter provide the necessary and sufficient information for approximating the polarizability of Eq. (2) using the frequencies and strengths $[\tilde{\epsilon}_i(n), \tilde{f}_i(n), i = 1, n]$ of Eqs. (22a), (22b) and (25) that provide principal representations^{25,26}

$$\tilde{S}(-k) = \sum_{i=1}^n \tilde{\epsilon}_i(n)^{-k} \tilde{f}_i(n), \quad k = 0, 1, \dots, 2n - 1 \quad (26)$$

of $2n$ spectral moments. In the case $n = M$, the original M frequencies $\tilde{\epsilon}_i(M) = \tilde{\epsilon}_i$ [Eq. (11a)] and strengths $\tilde{f}_i(M) = \tilde{f}_i$ [Eq. (13b)] are obtained from solution of Eq. (26), whereas, for $n \ll M$ the resulting $\tilde{\epsilon}_i(n)$ and $\tilde{f}_i(n)$ can give accurate approximations to the corresponding values $\epsilon_i(n)$ and $f_i(n)$ obtained from Eq. (26) employing the correct spectral sums $S(-k) [\cong \tilde{S}(-k), k < 2n]$ of Eq. (16b). A convergent smoothing of the discrete spectrum $[\tilde{\epsilon}_i, \tilde{f}_i, i = 1, M]$ is therefore obtained by noting that the $n\tilde{\epsilon}_i(n)$ and $\tilde{f}_i(n)$ values ($n \ll M$) furnish a histogram approximation to the cumulative oscillator-strength distribution in the form^{6,26}

$$\begin{aligned} f^{(n)}(\epsilon) &= 0, \quad 0 \leq \epsilon < \tilde{\epsilon}_1(n), \\ f^{(n)}(\epsilon) &= \sum_{i=1}^j \tilde{f}_i(n), \quad \tilde{\epsilon}_j(n) < \epsilon < \tilde{\epsilon}_{j+1}(n), \\ f^{(n)}(\epsilon) &= \sum_{i=1}^n \tilde{f}_i(n) = \tilde{S}(0), \quad \tilde{\epsilon}_n(n) < \epsilon, \end{aligned} \quad (27)$$

and to the differential oscillator-strength distribution from the Stieltjes derivative of Eq. (27) in the form^{6,26}

$$\begin{aligned} g^{(n)}(\epsilon) &= 0, \quad 0 \leq \epsilon \leq \tilde{\epsilon}_1(n), \\ g^{(n)}(\epsilon) &= \frac{1}{2} \frac{\tilde{f}_{j+1}(n) + \tilde{f}_j(n)}{\tilde{\epsilon}_{j+1}(n) - \tilde{\epsilon}_j(n)}, \quad \tilde{\epsilon}_j(n) < \epsilon < \tilde{\epsilon}_{j+1}(n), \\ g^{(n)}(\epsilon) &= 0, \quad \tilde{\epsilon}_n(n) < \epsilon. \end{aligned} \quad (28)$$

The cumulative distributions of successive orders

satisfy the Tchebycheff inequalities²⁶

$$f^{(n)}(\bar{\epsilon}_j(n) - 0) < f^{(n+1)}(\bar{\epsilon}_j(n) - 0) \leq f^{(n+1)}(\bar{\epsilon}_j(n) + 0) < f^{(n)}(\bar{\epsilon}_j(n) + 0) \quad (29)$$

at the points of increase $\bar{\epsilon}_j(n)$ of $f^{(n)}(\epsilon)$. [The notation $f^{(n)}(\bar{\epsilon}_j(n) \pm 0)$ refers to the right-hand/left-hand limit of $f^{(n)}(\epsilon)$ at $\bar{\epsilon}_j(n)$, respectively.] Moreover, the Stieltjes values of $f^{(n)}(\epsilon)$, defined according to

$$f^{(n)}(\bar{\epsilon}_j(n)) = \frac{1}{2} [f^{(n)}(\bar{\epsilon}_j(n) - 0) + f^{(n)}(\bar{\epsilon}_j(n) + 0)], \quad (30)$$

converge to $f(\epsilon)$ in the limit of large n . This is sufficient to ensure that the Stieltjes values of $g^{(n)}(\epsilon)$,

$$g^{(n)}(\bar{\omega}_j(n)) = \frac{1}{2} \frac{\bar{f}_{j+1}(n) + \bar{f}_j(n)}{\bar{\epsilon}_{j+1}(n) - \bar{\epsilon}_j(n)}, \quad (31a)$$

$$\bar{\omega}_j(n) = \frac{1}{2} [\bar{\epsilon}_{j+1}(n) + \bar{\epsilon}_j(n)], \quad (31b)$$

converge to $g(\epsilon)$ in the limit of large n .²⁷

Equations (26)–(31) provide convergent approximations to $f(\epsilon)$ and $g(\epsilon)$ at a finite number of frequency values, and thus image $f(\epsilon)$ and $g(\epsilon)$ in a subspace of the interval $0 \leq \epsilon < \infty$. In the limit of large n , when the correct spectral moments are employed, the image points become dense, and the complete functions are obtained from the Stieltjes values of the histograms [Eqs. (30), (31a), and (31b)]. Here, however, we have in mind the use of finite numbers of approximate moments. Consequently, it is convenient to employ the Stieltjes data points of Eqs. (30), (31a), and (31b) obtained from both upper and lower principal representations of Eq. (26) for a range of n values.²⁸ This procedure ensures that the points of increase $\bar{\epsilon}_i(n)$ obtained cover the important frequency interval uniformly. Appropriately chosen analytic forms $\bar{g}(\epsilon)$ and $\bar{f}(\epsilon)$ can be fitted to the total set of

TABLE I. Variational approximations to spectral sums in atomic helium.^a

k	$S(-k)$	k	$S(-k)$
0	1.992 526 7	10	4.388 329 7
1	1.504 771 0	11	5.432 192 3
2	1.383 018 9	12	6.760 420 0
3	1.414 911 1	13	8.450 108 0
4	1.542 067 1	14	10.600 006 3
5	1.749 848 5	15	13.336 510 9
6	2.040 660 7	16	16.821 358 5
7	2.426 460 2	17	21.261 497 0
8	2.926 767 8	18	26.921 739 6
9	3.568 743 0	19	34.140 980 3

^a Values in Hartree atomic units obtained from Eq. (16a) and a 90-term pseudospectrum [Eqs. (11a) and (11b)], as discussed in the text.

Stieltjes values [Eqs. (30), (31a), and (31b)] so constructed. Alternatively, one of the points of increase can be fixed at a specified frequency value [$\bar{\epsilon}_n(n) = \bar{\epsilon}$], and the remaining frequencies and strengths obtained uniquely from Eq. (26) using a fixed number $(2n - 1)$ of moments. The associated histograms [Eq. (27)] obtained in this fashion satisfy the Tchebycheff inequalities [Eq. (29)], and thus can be employed in the construction of Stieltjes values [Eq. (30)] at the specified frequency point $\bar{\epsilon}$. An appropriate analytic form $\bar{f}(\epsilon)$ can be fit to a large number of Stieltjes values so obtained, or the derivative curve $\bar{g}(\epsilon)$ can be constructed directly from finite differences.²⁹

The continuum oscillator-strength distribution is obtained directly from the approximation $\bar{g}(\epsilon)$ in the appropriate frequency interval, whereas, accurate approximations to the discrete f numbers are obtained from Eq. (31a) in the form

$$f_{i+1} + f_i = 2\bar{g}(\omega_i)(\epsilon_{i+1} - \epsilon_i), \quad (32)$$

where the ϵ_i are the correct transition frequencies, and $\omega_i = \frac{1}{2}(\epsilon_{i+1} + \epsilon_i)$. The resulting spectrum is then employed in evaluating the principal-value polarizability

$$\text{Re } \alpha(\omega) = \sum_{i=1}^{\infty} \frac{f_i}{\epsilon_i^2 - \omega^2} + P \int_{\epsilon_i}^{\infty} \frac{\bar{g}(\epsilon) d\epsilon}{\epsilon^2 - \omega^2}, \quad (33)$$

and the associated dispersion profiles of Sec. II.

TABLE II. Spectral sum rules and Cauchy moments in atomic helium.^a

Spectral sum	Present results ^b	Previous values
S(2)	12.1120	30.3325 ^c
S(1)	3.7690	4.0837 ^c
S(0)	1.9925	2.0000 ^d
S(-1)	1.5048	1.505 ^c
S(-2)	1.3830	1.3838 ^e
S(-4)	1.5421	1.5461 ± 0.0001 ^f
S(-6)	2.0407	2.042 ± 0.006 ^f
S(-8)	2.9268	2.95 ^e

^a All values in Hartree atomic units. The sum rules are discussed by J. O. Hirschfelder, W. Byers-Brown, and S. T. Epstein, *Adv. Quantum Chem.* **1**, 256 (1964), and R. Jackiw, *Phys. Rev.* **157**, 1220 (1967); the Cauchy moments by P. W. Langhoff and M. Karplus, *J. Chem. Phys.* **52**, 1435 (1970).

^b Values obtained from Eq. (16a) and a 90-term pseudospectrum [Eqs. (11a) and (11b)], as discussed in the text.

^c C. L. Pekeris, *Phys. Rev.* **112**, 1649 (1958).

^d Exact value from the f -sum rule.

^e P. W. Langhoff and M. Karplus, *J. Opt. Soc. Am.* **59**, 863 (1969).

^f G. Starkschall and R. G. Gordon, *J. Chem. Phys.* **54**, 663 (1971).

V. NUMERICAL RESULTS

A basis set of 60 functions formed from appropriate configurations of $1s-4s$, $1s'-3s'$, $2p$, and $3p$ orbitals with optimized Slater exponents, multiplied by Hylleraas correlation factors, is used to construct an approximate $^1S_0^e$ ground-state eigenfunction for atomic helium.³⁰ Similarly, 90 basis functions corresponding to both single and double excitations formed from appropriate configurations of $1s-6s$, $2p-9p$, and $3p'-5p'$ orbitals, multiplied by Hylleraas correlation factors, are used to con-

struct a $^1P_1^o$ pseudospectrum satisfying Eqs. (11a) and (11b). The nonlinear Slater exponents in the latter set of basis orbitals are distinct from those of the ground-state eigenfunction, and are optimized according to the energy lowering of the first excited state.³¹ Of the resulting $\tilde{\epsilon}_i$ and \tilde{f}_i values, the first three frequencies and strengths obtained are in good agreement with accurate values, although the higher frequencies are above the first ($n=1$) photoionization threshold. The presence of autoionizing states, additional (inelastic) photoionization thresholds ($n=2, 3, 4$), and the double

TABLE III. Frequencies and strengths that provide upper and lower principal representations of the atomic-helium spectral sums.^a

i	Upper principal representation ^b		Lower principal representation ^c	
	$\tilde{\epsilon}_i(10)$	$\tilde{f}_i(10)$	$\tilde{\epsilon}_i(10)$	$\tilde{f}_i(10)$
1	0.779 882 42	0.284 823 31	0.785 272 21	0.336 127 14
2	0.906 316 11	0.332 449 98	0.969 716 90	0.440 018 59
3	1.214 382 63	0.535 695 44	1.392 223 33	0.551 384 08
4	2.037 521 97	0.561 910 25	2.424 529 60	0.469 502 04
5	4.901 086 14	0.273 658 86	5.874 276 77	0.195 494 87
6	∞	0.003 988 89
	$\tilde{\epsilon}_i(13)$	$\tilde{f}_i(13)$	$\tilde{\epsilon}_i(13)$	$\tilde{f}_i(13)$
1	0.781 156 83	0.294 531 70	0.779 882 42	0.277 807 99
2	0.903 600 81	0.285 078 38	0.872 680 97	0.202 310 91
3	1.132 228 58	0.405 370 16	1.036 649 18	0.349 495 58
4	1.583 568 11	0.420 824 40	1.386 259 86	0.441 792 76
5	2.510 515 50	0.383 601 17	2.200 752 68	0.457 601 95
6	5.659 690 17	0.201 842 94	4.599 406 04	0.221 015 08
7	∞	0.001 277 98	8.656 417 21	0.042 502 46
	$\tilde{\epsilon}_i(16)$	$\tilde{f}_i(16)$	$\tilde{\epsilon}_i(16)$	$\tilde{f}_i(16)$
1	0.779 882 42	0.276 515 89	0.780 100 94	0.280 276 08
2	0.859 250 83	0.140 022 32	0.872 102 53	0.186 293 43
3	0.962 490 99	0.238 184 48	1.007 674 75	0.280 508 83
4	1.158 642 41	0.318 496 52	1.246 483 99	0.326 346 37
5	1.519 705 02	0.368 879 75	1.630 793 00	0.315 647 44
6	2.331 802 07	0.411 607 88	2.419 742 78	0.379 055 69
7	4.927 417 90	0.207 325 47	5.259 623 49	0.214 191 78
8	8.706 760 67	0.031 090 03	13.437 557 96	0.010 207 11
9	∞	0.000 404 39
	$\tilde{\epsilon}_i(19)$	$\tilde{f}_i(19)$	$\tilde{\epsilon}_i(19)$	$\tilde{f}_i(19)$
1	0.779 925 50	0.277 205 27	0.779 882 42	0.276 298 25
2	0.860 145 73	0.139 223 72	0.853 465 51	0.108 723 86
3	0.956 483 76	0.214 615 86	0.926 191 47	0.172 811 55
4	1.125 270 83	0.280 950 30	1.055 741 67	0.236 702 04
5	1.412 049 93	0.308 905 43	1.261 868 43	0.264 930 70
6	1.788 240 89	0.193 505 60	1.592 210 82	0.305 404 74
7	2.437 889 14	0.352 389 72	2.365 716 81	0.392 109 72
8	5.207 554 62	0.212 241 27	4.771 911 85	0.158 779 33
9	11.534 623 56	0.013 313 93	6.387 974 43	0.071 804 08
10	∞	0.000 175 63	17.302 759 91	0.004 962 46

^a Values in Hartree atomic units that provide principal representations [Eq. (26)] of the sums of Table I.

^b Obtained from Eq. (26) and the sums of Table I, setting $\tilde{\epsilon}_6(10) = \tilde{\epsilon}_7(13) = \tilde{\epsilon}_9(16) = \tilde{\epsilon}_{10}(19) = \infty$ and $\tilde{\epsilon}_1(10) = \tilde{\epsilon}_1(16) = \tilde{\epsilon}_1 = 0.779 882 42$ a.u.

^c Obtained from Eq. (26) and the sums of Table I, setting $\tilde{\epsilon}_1(13) = \tilde{\epsilon}_1(19) = \tilde{\epsilon}_1 = 0.779 882 42$ a.u.

ionization threshold are indicated in the pseudo-spectrum by stabilized or converging poles at the appropriate frequencies,^{1,9} discussed subsequently below.

The first 20 spectral moments obtained from the ground-state eigenfunction and the 90-term pseudo-spectrum are shown in Table I, and comparisons with previous theoretical, semiempirical, and experimental results are given in Table II. The $S(2)$ and $S(1)$ sums shown in Table II, which are not employed in the present development, are poor approximations to the accurate Pekeris values, since the basis set employed does not include the appropriate terms.³² The other sums are evidently in good agreement with previous values, suggesting that the results of Table I are an accurate reflection of the helium dipole spectrum, excluding the very-high-frequency region.

Transition frequencies and oscillator strengths that provide both upper and lower principal representations of between two and twenty of the sums of Table I are constructed from solutions of the appropriate moment equations [Eqs. (26)].²⁸ The Stieltjes values [Eqs. (30), (31a), and (31b)] of the 72 distinct histograms [Eqs. (27) and (28)] obtained provide approximately 200 data points for the cumulative distribution $f(\epsilon)$, and 200 data points for the differential distribution $g(\epsilon)$. As an illustration, the frequencies and strengths that pro-

vide principal representations of 10, 13, 16, and 19 of the sums of Table I are shown in Table III. The values obtained from the lower principal representations of 10 and 16 sums also result from explicit transformation to a principal basis set [Eqs. (21)–(25)] of five or eight pseudostates, respectively. In Figs. 1 and 2 are shown four of the 12 histograms obtained from the principal transition frequencies and oscillator strengths of Table III. Also shown in the figures are Stieltjes values of lower-order histograms obtained employing fewer moments than the 13 and 16 moments appropriate for the frequencies and strengths of Table III. In Fig. 1, approximately 70 of the 85 Stieltjes data points obtained using between 10 and 13 sums are shown, whereas, in Fig. 2, Stieltjes data points obtained from between 13 and 16 sums are shown. Comparison of Figs. 1 and 2, and careful examination of the additional histograms constructed (not shown), suggests that the Stieltjes values obtained from representations of between 10 and 20 of the sums of Table I are convergent to smooth profiles. Moreover, the large number of data points obtained from the upper and lower principal representations suggests that the histograms associated with additional fixed-point quasiorthogonal polynomials are not required in atomic helium.

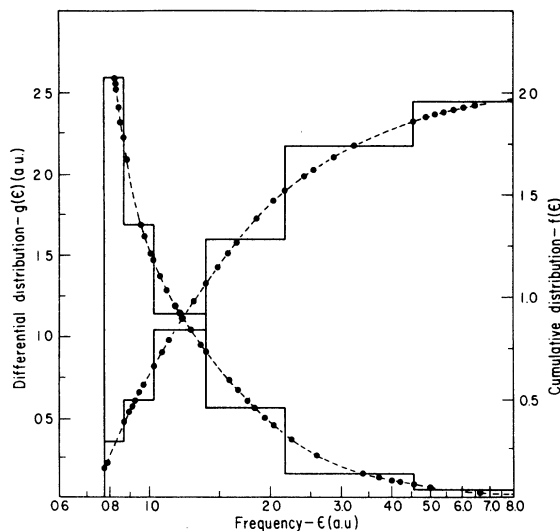


FIG. 1. Differential and cumulative oscillator-strength distributions in atomic helium; solid line (—), Stieltjes histograms [Eqs. (27) and (28)] obtained from the frequencies and strengths (Table II) that provide a lower principal representation of 13 spectral sums (Table I); selected Stieltjes values (●) [Eqs. (30), (31a), and (31b)] obtained from principal representations of between 10 and 13 spectral sums (Table I); dashed line (---), fifth-order polynomial in $1/\epsilon$ fitted to Stieltjes data.

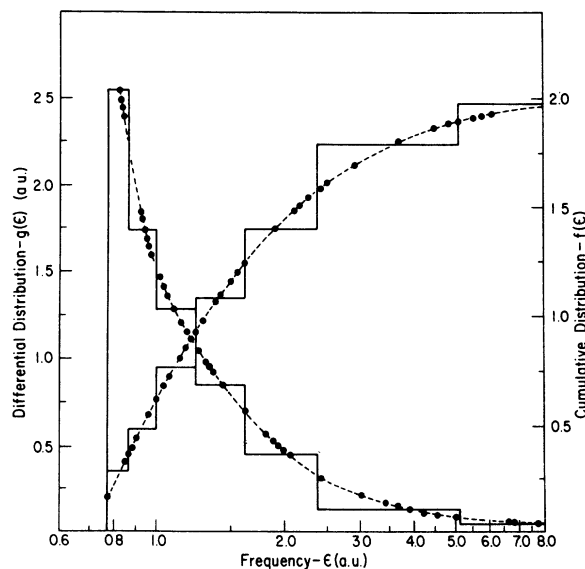


FIG. 2. Differential and cumulative oscillator-strength distributions in atomic helium; solid line (—), Stieltjes histograms [Eqs. (27) and (28)] obtained from the frequencies and strengths (Table II) that provide a lower principal representation of 16 spectral sums (Table I); selected Stieltjes values (●) [Eqs. (30), (31a), and (31b)] obtained from principal representations of between 13 and 16 spectral sums (Table I); dashed line (---), fifth-order polynomial in $1/\epsilon$ fitted to Stieltjes data.

TABLE IV. Mean-square deviations of fifth-order polynomial fit to Stieltjes data for atomic helium.^a

Number of moments ^b	Number of data points ^c		Mean-square deviation ^d	
	$g(\epsilon)$	$f(\epsilon)$	$g(\epsilon)$	$f(\epsilon)$
10	8	10	2.58×10^{-4}	1.93×10^{-5}
10-13	38	46	2.80×10^{-4}	2.34×10^{-5}
10-16	77	91	3.78×10^{-4}	3.34×10^{-5}
10-20	143	165	10.58×10^{-4}	10.38×10^{-5}

^a Mean-square deviations in Hartree atomic units appropriate for the polynomials

$$\tilde{g}(\epsilon) = \sum_{j=0}^5 a_j \left(\frac{1}{\epsilon}\right)^j, \quad \tilde{f}(\epsilon) = \sum_{j=0}^5 b_j \left(\frac{1}{\epsilon}\right)^j$$

fitted to the indicated numbers of Stieltjes data points [Eqs. (30), (31a), and (31b)].

^b Number of spectral sums of Table I employed.

^c Numbers of Stieltjes data points [Eqs. (30), (31a), and (31b)] obtained from histograms [Eqs. (27) and (28)] constructed with indicated spectral sums.

^d Deviations constructed in the customary manner.

Polynomials in $(1/\epsilon)$ fitted to the Stieltjes values provide convenient analytic forms which accurately approximate the cumulative and differential oscillator-strength distributions in atomic helium. In Table IV are shown the mean-square deviations appropriate for fifth-order polynomials in $(1/\epsilon)$ fit to various Stieltjes values.³³ The smooth pro-

files $\tilde{g}(\epsilon)$ and $\tilde{f}(\epsilon)$ obtained in this way from the various data sets are in excellent mutual agreement, differing by less than a few parts in the third significant figure in the interval $\epsilon_1 \leq \epsilon < 10$ a.u., and the mean-square deviations of Table IV evidently show very little increase as greater numbers of data points are used. The very small scat-

TABLE V. Discrete oscillator strengths in atomic helium.^a

Transition frequencies ^b	Oscillator strengths	
	Present results ^c	Previous values
0.7797, [0.7799]	0.276 26	0.2761 ± 0.0014 , ^d 0.2762 ^e
0.8484, [0.8486]	0.7330(-1)	$0.735 \pm 0.036(-1)$, ^d 0.73(-1) ^e
0.8725, [0.8727]	0.2994(-1)	$0.303 \pm 0.071(-1)$, ^d 0.30(-1) ^e
0.8836	0.156(-1)	$0.1481(-1)$, ^f 0.153(-1) ^g
0.8897	0.900(-2)	$0.841(-2)$, ^f 0.878(-2) ^g
0.8934	0.564(-2)	$0.518(-2)$ ^f
0.8958	0.378(-2)	$0.340(-2)$ ^f
0.8974	0.265(-2)	$0.264(-2)$ ^h
0.8986	0.193(-2)	$0.193(-2)$ ^h
0.8994	0.145(-2)	$0.145(-2)$ ^h

^a Hartree atomic units are employed. Values in parenthesis indicate appropriate powers of ten.

^b C. E. Moore, *Atomic Energy Levels*, Natl. Bur. Std. Circ. No. 467 (U.S. GPO Washington, D. C. 1949), Vol. I. Values in brackets obtained from variational calculations [Eqs. (11a) and (11b)] as discussed in the text.

^c Strengths of the first three transitions obtained from variational calculations [Eqs. (11a), (11b), and (13b)] as discussed in the text. Other strengths obtained from Eq. (32), $\tilde{g}(\epsilon)$ fit to the Stieltjes data of Figs. 1 and 2, and $f_{19} = 0.2409(-3)$ obtained from the Coulomb approximation (see footnote h).

^d M. T. Anderson and F. Weinhold, *Phys. Rev. A* **9**, 118 (1974).

^e B. Schiff and C. L. Pekeris, *Phys. Rev.* **134**, A638 (1964).

^f L. C. Green, N. C. Johnson, and E. K. Kolchin, *Astrophys. J.* **144**, 369 (1966).

^g A. Dalgarno and A. L. Stewart, *Proc. Phys. Soc. Lond.* **76**, 49 (1960).

^h Values obtained from the Coulomb approximation of J. Hargreaves, *Proc. Camb. Philos. Soc.* **25**, 91 (1928); A. Burgess and M. T. Seaton, *Mon. Not. R. Astron. Soc.* **120**, 121 (1960), using $\tilde{g}(\epsilon_i) = 1.927$ obtained from the Stieltjes procedure.

ter evident in the Stieltjes values, and the stability of simple fifth-order polynomials fit to the data points, indicates that convergence has indeed been achieved using between 10 and 20 of the sums of Table I. Even the lower-order data obtained from between five and ten moments (not shown) are in excellent agreement with the smooth profiles obtained from between 10 and 20 spectral sums.

In Table V are shown the Stieltjes approximations to the discrete oscillator strengths in atomic helium obtained from Eq. (32) and the fifth-order polynomial fit to the Stieltjes data of Figs. 1 and 2. These data fits are chosen for this purpose in view of the remarkably small mean-square deviations obtained for both $\tilde{g}(\epsilon)$ and $\tilde{f}(\epsilon)$ (Table IV). In addition, the derivative of $\tilde{f}(\epsilon)$ differs from $\tilde{g}(\epsilon)$ by less than 1% over the discrete frequency interval, and the transition frequencies obtained from the other polynomial fits of Table IV differ from the values of Table V by no more than a few parts in the third significant figure. Evidently, the Stieltjes results of Table V, which are expected to be accurate to at least 5%, are in excellent agreement with those of the Coulomb approximation³⁴ very near the photoionization threshold, and are also in excellent agreement with experimental and previously obtained theoretical values for the lower resonance transitions.⁴

The Stieltjes results of Table V and the associated approximation $\tilde{g}(\epsilon)$ to the photoionization profile are used in the evaluation of the absorption and dispersion profiles shown in Fig. 3. Values of Eq. (33) obtained employing the other data fits of Table IV differ from the results of Fig. 3 by a few percent, indicating a moderate sensitivity of the dispersion profile to the absorption spectrum employed in its evaluation. Note, however, that the polarizability in the normal dispersion interval does not require Eq. (33), but rather is evaluated directly from the points and weights of Table III and Eq. (13a). The principal-value polarizability has a minimum in the photoionization continuum apparently as a consequence of the relatively large contribution the photoionization profile makes to the f -sum rule (~ 1.56). Evidently, the Stieltjes results are in good accord with the experimental photoabsorption³⁵ and refractivity³⁶ data.

More detailed comparisons of the Stieltjes results with the experimental photoabsorption and refractivity data are given in Tables VI and VII, respectively. The photoabsorption data of Table VI is in very good agreement with the Stieltjes values in the threshold region and at higher frequencies, whereas, in the interval from ~ 1.3 – 2.4 a.u. the experimental data is uniformly below the present results. However, the Stieltjes values are generally within the $\pm 10\%$ estimated error for

the measured absorption index.³⁵ Similarly, the experimental refractivity³⁶ values of Table VII are in excellent agreement with the Stieltjes results. It is of particular significance to note that the previously obtained moment-theory bounds, which employ the $S(2)$ to $S(-2)$ sums,⁸ are in excellent agreement with the Stieltjes results.

In Table VIII are shown the Stieltjes results for the Verdet coefficient and Rayleigh-scattering cross section, in comparison with previous moment-theory bounds,⁸ experimental values,³⁷ and estimates obtained from Eq. (6) using experimental refractivities for the polarizability. All three independent sets of values obtained for both the Verdet coefficient and the Rayleigh-scattering cross section are evidently in very good mutual agreement.

Although a detailed investigation of autoionizing line shapes and inelastic thresholds in the dipole spectrum of atomic helium is beyond the scope of the present investigation,³⁸ it is of considerable interest to examine the variationally determined pseudospectrum of discrete transition frequencies and oscillator strengths for the presence of such

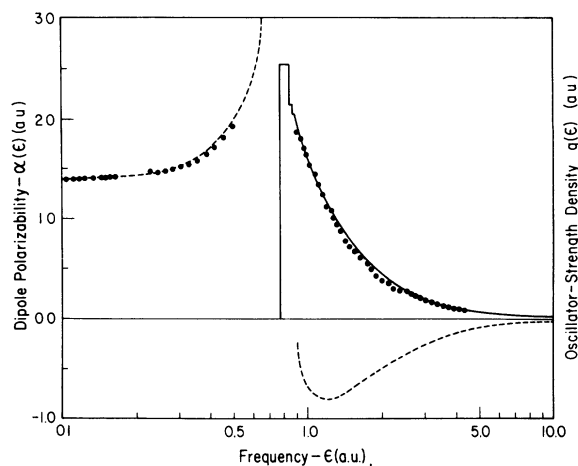


FIG. 3. Dipole oscillator-strength distribution and polarizability in atomic helium; solid line (—), Stieltjes values for the oscillator-strength distribution obtained from Eqs. (31a), (31b), and (32) and the data of Figs. 1 and 2 as discussed in the text; dashed line (---), Stieltjes values for the polarizability obtained from Eq. (13a) and the data of Table III in the normal dispersion interval, and from Eq. (33) and the associated absorption profile in the photoionization interval, as discussed in the text; closed circle (●), experimental values; absorption data from J. A. R. Samson, *Adv. At. Mol. Phys.* **2**, 178 (1966) and J. F. Lowry, D. H. Tomboulian, and D. L. Ederer, *Phys. Rev.* **135**, A1054 (1965); refractivity data from C. Cuthbertson and M. Cuthbertson, *Proc. R. Soc. Lond.* **135**, 40 (1932); C. R. Mansfield and E. R. Peck, *J. Opt. Soc. Am.* **59**, 199 (1969), and M. C. E. Huber and G. Tondello, *J. Opt. Soc. Am.* **64**, 390 (1974).

features. In Table IX are shown the first 30 variationally determined frequencies and strengths, the associated approximation to the continuum photoionization oscillator-strength density [Eq. (31a)], and the corresponding Stieltjes results of Figs. 1 and 2. As indicated above, the first three $\bar{\epsilon}_i$ and \bar{f}_i values are in good accord with accurate results (Table V), whereas, the two subsequent $\bar{\epsilon}_i$ and \bar{f}_i , although below the elastic ionization threshold ($\epsilon_i \cong 0.904$ a.u.), do not correspond directly to any of the correct discrete transitions in atomic helium. The $\bar{\epsilon}_i$ and \bar{f}_i values in the interval 0.9270–1.347 a.u. simulate the elastic (one-particle) photoionization profile, and the associated density $g(\epsilon)$ obtained directly from Eq. (31a) is evidently in good agreement with the accurate Stieltjes results. Above the $2s2p$ double-excitation

threshold (~ 2.21 a.u.) the spacings of the variational transition frequencies are considerably smaller than in the one-particle-only ionization interval, indicating the presence of pseudostates that correspond to two-electron excitations. Moreover, the $2s2p$ line shape is qualitatively suggested by a significant peak in the variational approximation to the photoionization profile at ~ 2.30 a.u., and the $n=2$ inelastic photoionization threshold (~ 2.40 a.u.) is indicated by clustered eigenvalues at the appropriate position. There is evidently no simple connection between the variational and Stieltjes distributions $g(\epsilon)$, however, above the $2s2p$ excitation, and additional techniques are required in order to obtain quantitative estimates for the contributions of the various photoionization channels to the total profile.³⁹

TABLE VI. Absorption index in atomic helium.^a

Wavelength λ (Å)	Experimental values ^b	Present results ^c	Wavelength λ (Å)	Experimental values ^b	Present results ^c
100.9	12.9	8.87	215.2	39.4	42.1
107.0	9.8	9.92	220.4	40.5	44.4
115.8	9.6	11.5	225.2	38.6	46.5
117.9	11.0	11.9	231.2	42.7	49.2
122.3	12.2	12.8	247.2	53.0	56.7
125.2	14.9	13.4	283.6	66.0	74.9
128.3	13.4	14.0	303.1	78.0	84.9
131.8	13.9	14.8	315.0	79.0	91.1
132.8	14.2	15.1	323.2	85.0	95.3
135.5	15.1	15.7	335.4	99.0	102
139.0	16.0	16.5	345.0	101	106
144.8	19.6	17.9	357.5	108	113
151.5	19.0	19.7	364.0	113	116
156.2	22.1	21.0	375.7	120	122
160.1	21.9	22.1	390.6	132	130
164.6	23.5	23.5	397.1	133	133
168.1	23.8	24.5	405.7	140	138
171.1	24.4	25.5	416.6	148	143
177.8	25.6	27.7	425.5	157	148
182.4	28.4	29.3	436.5	160	155
185.7	30.2	30.5	448.8	166	163
192.8	29.2	33.1	464.4	174	173
198.0	31.9	35.1	478.0	184	184
202.3	32.9	36.8	489.3	191	194
207.2	41.9	38.8	503.0	198	208

^a Values in cm^{-1} appropriate for Eq. (1a), with $(4\pi N_0/c) \cong 69.02$ and $\omega \text{Im}\alpha(\omega)$ in Hartree atomic units. To convert wavelength in angstrom units to frequency in atomic units, use $\omega(\text{a.u.}) \cong 455.6/\lambda(\text{Å})$.

^b Data in the interval 215.2–503.0 Å taken from J. A. R. Samson, *Adv. At. Mol. Phys.* **2**, 178 (1966), and in the interval 100.9–207.2 Å taken from J. F. Lowry, D. H. Tomboulian, and D. L. Ederer, *Phys. Rev.* **137**, A1054 (1965). Selected data points taken from the tabulated values in each case.

^c Values obtained from the Stieltjes procedure employing the profiles of Figs. 1 and 2 as discussed in the text. Previous theoretical determinations cited in Ref. 4 are in good accord with the present results.

VI. CONCLUDING REMARKS

A previously described Stieltjes-imaging technique⁶ is employed in the *ab initio* calculation of dipole absorption and dispersion profiles in atomic helium. Variationally determined square-integrable pseudostates having appropriate symmetry provide the dipole spectral sums and principal eigenstates, frequencies, and strengths necessary for construction of the profiles. The Stieltjes

TABLE VII. Dispersion of the refractive index in atomic helium.^a

Wavelength λ (Å)	Refractivity $[\tilde{n}(\omega) - 1] \times 10^6$		
	Experimental values ^b	Moment-theory bounds ^c	Present results ^d
9660	34.76	34.71 ± 0.01	34.69
9227	34.77	34.72 ± 0.01	34.70
9125	34.78	34.72 ± 0.01	34.70
8267	34.80	34.74 ± 0.01	34.72
7247	34.83	34.78 ± 0.02	34.76
5462	34.95	34.89 ± 0.04	34.87
5087	35.00	34.94 ± 0.04	34.92
4801	35.04	34.97 ± 0.05	34.95
4359	35.05	35.05 ± 0.06	35.03
4047	35.12	35.12 ± 0.07	35.10
3664	35.23	35.23 ± 0.08	35.21
3342	35.36	35.36 ± 0.10	35.34
3132	35.47	35.46 ± 0.11	35.44
3022	35.53	35.52 ± 0.12	35.51
2926	35.59	35.59 ± 0.13	35.57
2753	35.73	35.72 ± 0.15	35.70
1900	37.7	37.00 ± 0.36	37.01
1800	37.3	37.30 ± 0.41	37.31
1700	37.4	37.66 ± 0.47	37.67
1600	37.8	38.10 ± 0.55	38.11
1500	38.3	38.65 ± 0.65	38.66
1400	38.9	39.34 ± 0.79	39.37
1300	39.6	40.25 ± 0.97	40.28
1200	40.7	41.46 ± 1.24	41.51
1100	42.6	43.16 ± 1.66	43.22
1000	45.3	45.67 ± 2.34	45.77
920	48.5	48.72 ± 3.30	48.86

^a The refractivity of Eq. (1b) is dimensionless, with $2\pi N_0 \cong 0.2502 \times 10^{-6}$ at STP (0 °C, 1 atm) and $\text{Re}(\alpha(\omega))$ in Hartree atomic units.

^b Values in the interval 9600 to 4801 Å taken from C. R. Mansfield and E. R. Peck, *J. Opt. Soc. Am.* **59**, 199 (1969), who suggest an absolute error of ±0.09, in the interval 4359 to 2753 Å from C. Cuthbertson and M. Cuthbertson, *Proc. R. Soc.* **135**, 40 (1932), and in the interval 1900 to 920 Å from M. C. E. Huber and G. Tondello, *J. Opt. Soc. Am.* **64**, 390 (1974), who suggest a probable error of ~±3%.

^c P. W. Langhoff, *Chem. Phys. Lett.* **9**, 89 (1971); *J. Chem. Phys.* **57**, 2604 (1972).

^d Values obtained from the Stieltjes-imaging technique described in the text and the sums of Table I. Previous theoretical determinations cited in Ref. 5 are in good accord with the present results.

TABLE VIII. Dispersion of the Verdet coefficient and Rayleigh-scattering cross section in atomic helium.^a

Wavelength λ (Å)	Experimental values ^b	Moment-theory bounds ^c	Present results ^d
Verdet coefficient $V(\omega)$			
9000	0.203	0.200 ± 0.026	0.201
8500	0.221	0.224 ± 0.029	0.225
8000	0.246	0.253 ± 0.033	0.254
7500	0.283	0.288 ± 0.038	0.290
7000	0.325	0.332 ± 0.043	0.333
6500	0.379	0.385 ± 0.051	0.387
6000	0.441	0.453 ± 0.060	0.455
5893	0.457	0.470 ± 0.062	0.472
5780	0.474	0.489 ± 0.065	0.491
5500	0.522	0.540 ± 0.072	0.543
5460	0.530	0.549 ± 0.073	0.551
5000	0.637	0.657 ± 0.088	0.660
4500	0.800	0.815 ± 0.110	0.819
4360	0.853	0.870 ± 0.118	0.874
4000	1.011	1.039 ± 0.142	1.044
3635	1.253	1.268 ± 0.175	1.273
Rayleigh cross section $\sigma(\omega) \times 10^{28}$			
9227	0.0764	0.0761 ± 0.0000	0.0760
8267	0.119	0.118 ± 0.000	0.118
7247	0.201	0.201 ± 0.000	0.201
5462	0.628	0.626 ± 0.001	0.626
4801	1.058	1.054 ± 0.003	1.053
4359	1.558	1.558 ± 0.005	1.556
4047	2.105	2.104 ± 0.008	2.103
3664	3.153	3.153 ± 0.014	3.150
3132	5.986	5.980 ± 0.038	5.977
2753	10.18	10.17 ± 0.085	10.16
1900	49.9	48.10 ± 0.94	48.12
1700	76.7	77.75 ± 1.94	77.79
1500	133	135.1 ± 4.5	135.2
1300	251	259.7 ± 12.5	260.1
1100	567	582.5 ± 44.8	584.1
920	1500	1517 ± 206	1526

^a The Verdet coefficient of Eq. (7) is in units of $\mu \text{ min} / \text{Oe cm-atm}$, with $\frac{1}{2}c^2 \cong 1.007$ and $\omega \text{ dn}(\omega) / d\omega$ dimensionless, and the Rayleigh-scattering cross section of Eq. (6) is in units of cm^2 , with $(24\pi/9)(1/c)^4 \cong 6.652 \times 10^{-25}$ and $\omega^4 \text{Re}(\alpha(\omega)^2)$ in Hartree atomic units.

^b Verdet-coefficient data from L. R. Ingersoll and D. H. Liebenberg, *J. Opt. Soc. Am.* **46**, 538 (1956). Rayleigh-scattering cross section obtained from Eq. (6) and the experimental refractivity data of Table VII.

^c P. W. Langhoff, *Chem. Phys. Lett.* **9**, 89 (1971); *J. Chem. Phys.* **57**, 2604 (1972).

^d Values obtained from the Stieltjes-imaging technique described in the text and the sums of Table I. The coupled Hartree-Fock calculations of the Verdet coefficient by V. G. Kaveeshwar, K. T. Chung, and R. P. Hurst, *Phys. Rev.* **172**, 35 (1968), are in good accord with the present results.

TABLE IX. Variationally determined pseudospectrum in atomic helium.^a

Frequencies ξ_i	Strengths \tilde{f}_i	Oscillator-strength distribution $g(\epsilon)$	
		Variational results ^b	Stieltjes results ^c
0.779 88	0.276 255
0.848 58	0.073 299
0.872 66	0.029 935
0.885 08	0.022 374
0.900 53	0.037 127
0.927 04	0.059 718	1.727	1.712
0.970 93	0.091 901	1.571	1.520
1.043 91	0.137 448	1.324	1.301
1.166 99	0.188 395	1.029	1.064
1.346 99	0.182 141	0.851	0.808
1.609 36	0.264 292	0.224	0.468
2.275 70	0.034 380	1.080	0.322
2.337 41	0.098 991	6.637	0.309
2.362 30	0.231 321	4.223	0.302
2.391 42	0.014 665	0.909	0.296
2.399 83	0.000 610	0.018	0.293
2.418 91	0.000 086	0.013	0.287
2.443 55	0.000 552	0.017	0.280
2.472 83	0.000 442	0.012	0.274
2.492 70	0.000 025	0.007	0.268
2.524 82	0.000 440	0.014	0.260
2.562 56	0.000 609	0.015	0.253
2.588 07	0.000 178	0.003	0.245
2.636 77	0.000 120	0.003	0.237
2.673 67	0.000 090	0.001	0.229
2.723 15	0.000 004	0.000	0.221
2.757 96	0.000 012	0.000	0.211
2.846 97	0.000 012	0.006	0.200
2.899 77	0.000 647	0.038	0.193
2.944 29	0.002 756	0.025	0.184

^a All values in Hartree atomic units. The ξ_i and \tilde{f}_i are obtained from variational calculation [Eqs. (11)–(13)], as discussed in the text.

^b Values obtained from the ξ_i and \tilde{f}_i and Eq. (31a).

^c Stieltjes profile of Figs. 1 and 2 obtained as discussed in the text.

results are found to be in excellent agreement with experimental values and/or previously obtained theoretical estimates of the absorption coefficient, refractive index, Verdet coefficient, shielding factor, and Rayleigh-scattering cross section. In view of the relatively conventional nature of the computations required, and of the explicit avoidance of eigenstates with scattering boundary conditions, it can be anticipated that the Stieltjes approach will also prove useful in determinations of the absorption and dispersion profiles of more complex systems.

ACKNOWLEDGMENTS

Acknowledgment is made to the National Science Foundation and to the donors of The Petroleum Research Fund, administered by the American Chemical Society, for partial support of this work. It is a pleasure to thank W. P. Reinhardt, G. A. Baker, Jr., K. B. Winterbon, F. Weinhold, and J. M. Combes for helpful conversation and correspondence, and to thank V. McKoy and co-workers for providing preprints of their work prior to publication.

*Work supported in part by grants from The Petroleum Research Fund, administered by the American Chemical Society, and the National Science Foundation.

¹U. Fano and J. W. Cooper, *Rev. Mod. Phys.* **40**, 441 (1968).

²G. Breit, in *Encyclopaedic Dictionary of Physics*, edited by J. Thewlis (Pergamon, London, 1962).

³B. W. Shore, *Rev. Mod. Phys.* **39**, 439 (1967).

⁴H. A. Bethe and E. E. Salpeter, *Quantum Mechanics of One- and Two-Electron Atoms* (Springer-Verlag,

- Berlin, 1957). Explicit calculations in the case of atomic helium are given, for example, by B. Schiff and C. L. Pekeris, *Phys. Rev.* **134**, A638 (1964); L. C. Green, N. C. Johnson, and E. K. Kolchin, *Astrophys. J.* **144**, 369 (1966); M. T. Anderson and F. Weinhold, *Phys. Rev. A* **9**, 118 (1974), for discrete dipole excitations; and by P. G. Burke and D. D. McVicar, *Proc. Phys. Soc. Lond.* **86**, 989 (1965); K. L. Bell and A. E. Kingston, *Proc. Phys. Soc. Lond.* **90**, 31 (1967); and V. Jacobs, *Phys. Rev. A* **3**, 289 (1971), for the photoionization profile.
- ⁵A. Dalgarno, in *Perturbation Theory and Its Applications in Quantum Mechanics*, edited by C. H. Wilcox (Wiley, New York, 1966); P. W. Langhoff, S. T. Epstein, and M. Karplus, *Rev. Mod. Phys.* **44**, 602 (1972). Explicit variational calculations of the normal dispersion profile in atomic helium are given, for example, by Y. M. Chan and A. Dalgarno, *Proc. Phys. Soc. Lond.* **85**, 227 (1965); and K. T. Chung, *Phys. Rev.* **166**, 1 (1968).
- ⁶P. W. Langhoff, *Chem. Phys. Lett.* **22**, 60 (1973); P. W. Langhoff and C. T. Corcoran, *J. Chem. Phys.* **61**, 146 (1974).
- ⁷A. Dalgarno, *Rev. Mod. Phys.* **35**, 522 (1963).
- ⁸P. W. Langhoff, *Chem. Phys. Lett.* **9**, 89 (1971); *J. Chem. Phys.* **57**, 2604 (1972).
- ⁹R. P. Madden and K. Codling, *Astrophys. J.* **141**, 364 (1965).
- ¹⁰G. V. Marr, *Photoionization Processes in Gases* (Academic, New York, 1967), pp. 7 and 33.
- ¹¹S. A. Korff and G. Breit, *Rev. Mod. Phys.* **4**, 471 (1932).
- ¹²See, for example, J. C. Slater, *Quantum Theory of Atomic Structure* (McGraw-Hill, New York, 1960), Vol. I, p. 154.
- ¹³V. G. Kaveeshwar, A. Dalgarno, and R. P. Hurst, *J. Phys. B* **2**, 984 (1969).
- ¹⁴I. L. Fabelinski, *Molecular Scattering of Light* (Plenum, New York, 1968).
- ¹⁵J. H. Van Vleck, *The Theory of Electric and Magnetic Susceptibilities* (Oxford, London, 1932), p. 367.
- ¹⁶A. Dalgarno, *Adv. Chem. Phys.* **12**, 143 (1967); P. W. Langhoff and M. Karplus, in *The Padé Approximant in Theoretical Physics*, edited by G. A. Baker, Jr. and J. L. Gammel (Academic, New York, 1970), pp. 41–97.
- ¹⁷P. W. Langhoff and A. C. Yates, *Phys. Rev. Lett.* **25**, 1317 (1970); *J. Phys. B* **5**, 1071 (1972).
- ¹⁸J. O. Hirschfelder, W. Byers-Brown, and S. T. Epstein, *Adv. Quantum Chem.* **1**, 256 (1964).
- ¹⁹H. J. Kolker and H. H. Michels, *J. Chem. Phys.* **43**, 1027 (1965).
- ²⁰M. Karplus and H. J. Kolker, *J. Chem. Phys.* **39**, 1493 (1963).
- ²¹P. W. Langhoff and M. Karplus, *J. Chem. Phys.* **52**, 1435 (1970).
- ²²Physically significant autoionizing states and inelastic thresholds imbedded in the continuum are evident in the pseudospectrum, however, when an appropriate basis set is employed. This structure is further discussed in Sec. V. See also A. U. Hazi and H. S. Taylor, *Phys. Rev. A* **1**, 1109 (1970); G. V. Nazarov, *Int. J. Quantum Chem.* **6**, 87 (1972).
- ²³P. W. Langhoff and M. Karplus, *J. Opt. Soc. Am.* **59**, 863 (1969).
- ²⁴C. Tavaud, *C. R. Acad. Sci. (Paris)* **268**, 773 (1969).
- ²⁵S. J. Karlin and W. J. Studden, *Tchebycheff Systems* (Interscience, New York, 1966).
- ²⁶J. A. Shohat and J. D. Tamarkin, *The Problem of Moments* (American Mathematical Society, Providence, 1943).
- ²⁷The convergence is assured when the correct moments [Eq. (16b)] are used, whereas, with approximate moments [Eq. (16a)] the convergence of the Stieltjes values [Eqs. (30), (31a), and (31b)] will fail for $n > M$. That is, as indicated in the text, for $n=M$ the original discrete spectrum $[\xi_i, \tilde{f}_i, i=1, M]$ is recovered from Eq. (26), and for $n > M$ there are no additional solutions of the moment equations. Consequently, when approximate moments are used, the Stieltjes approach can be characterized as a smoothing technique, and in this connection is similar to the method of J. T. Broad and W. P. Reinhardt, *J. Chem. Phys.* **60**, 2182 (1974); and T. N. Rescigno, C. W. McCurdy, Jr., and V. McCoy, *Phys. Rev.* **9**, 2409 (1974), who explicitly continue an approximate polarizability in the form of Eq. (13a) from complex values to the real axis with an $[n, n]$ rational fraction. Additional techniques employing polarizabilities of the form of Eq. (13a) in the determination of absorption profiles are described by A. Dalgarno, H. Doyle, and M. Oppenheimer, *Phys. Rev. Lett.* **29**, 1051 (1972); and G. W. F. Drake, *Astrophys. J.* **184**, 145 (1973).
- ²⁸The upper and lower principal representations of both even and odd numbers of moments, having frequency points fixed at the lower and/or upper end of the interval $[\epsilon_1, \infty)$, are described concisely by J. C. Wheeler and R. G. Gordon, in *The Padé Approximant in Theoretical Physics*, edited by G. A. Baker, Jr. and J. L. Gammel (Academic, New York, 1970), pp. 99–128. See also G. Starkschall and R. G. Gordon, *J. Chem. Phys.* **54**, 663 (1971), and Ref. 8 and additional references cited therein.
- ²⁹In principal, it is possible to obtain explicit analytical expressions for the frequencies and strengths of the histogram having a point at ϵ from the associated quasiorthogonal polynomial (Ref. 26, Corollary 25, p. 45). In the present development, high-order polynomials are encountered, and the resulting analysis becomes cumbersome, making a numerical approach somewhat more convenient. It is interesting to note, however, that the analytic expressions obtained in this way for the cumulative and differential oscillator-strength distributions are rational fractions of the forms employed by W. P. Reinhardt and co-workers in their numerical continuation approach (Ref. 27). Consequently, the histograms having fixed points of increase associated with quasiorthogonal polynomials provide a justification for a *a priori* choice of rational fractions in the numerical continuation technique, and presumably give a basis for establishing convergence. For a closely related discussion in the case of analytic continuation of elastic scattering Fredholm determinants, which does not make explicit use of the fixed-point quasiorthogonal polynomials, however, see P. W. Langhoff and W. P. Reinhardt, *Chem. Phys. Lett.* **24**, 495 (1973). We are most grateful to both G. A. Baker, Jr. and K. B. Winterbon for independently urging us to employ the distributions associated with quasi-orthogonal polynomials having specified roots other

than those of the upper and lower representations; see K. B. Winterbon, *J. Chem. Phys.* 53, 1302 (1970), for applications in another area,

³⁰Computational details are described separately by J. Sims (unpublished). The lowest eigenvalue obtained is -2.90372399 a.u., compared with -2.90372435 a.u., obtained by C. L. Pekeris, *Phys. Rev.* 112, 1649 (1958).

³¹The lowest $^1P_1^o$ eigenvalue obtained is -2.12384194 a.u., compared with the recent value of -2.12384303 a.u., obtained by M. T. Anderson and F. Weinhold (Ref. 4).

³²A. Dalgarno and S. T. Epstein, *J. Chem. Phys.* 50, 2837 (1969). We are informed by F. Weinhold that including the terms necessary for satisfying the $S(2)$ and $S(1)$ sum rules, which requires the evaluation of special integrals, improves the convergence of the other sums, as well. In order to demonstrate that the Stieltjes technique can provide satisfactory results employing conventional configuration-interaction calculations, the necessary special trial functions are not included in the present development, and are considered separately in a subsequent publication.

³³Higher-order polynomials in $(1/\epsilon)$, and other functional forms, can also be employed in the fitting procedure. For example, in the case of the 10-16 moment data, the use of tenth-order polynomials gives mean-square deviations of 2.10×10^{-4} and 1.33×10^{-5} for $\bar{g}(\epsilon)$ and $\bar{f}(\epsilon)$, respectively, compared with 3.78×10^{-4} and 3.34×10^{-5} from Table IV. Careful examination of the higher-order profiles reveals the presence of small oscilla-

tions, however, indicating that fifth-order polynomials are more appropriate for smoothing the data points available in atomic helium. Other photoionization profiles may require the use of more elaborate functional forms, in which cases the quasiorthogonal polynomials with fixed frequency points can provide a useful alternative approach to a fitting procedure. The latter are considered in more detail in a subsequent publication.

³⁴J. Hargreaves, *Proc. Camb. Philos. Soc.* 25, 91 (1928); A. Burgess and M. T. Seaton, *Mon. Not. R. Astron. Soc.* 120, 121 (1960).

³⁵J. A. R. Samson, *Adv. At. Mol. Phys.* 2, 178 (1966); J. F. Lowry, D. H. Tomboulion, and D. L. Ederer, *Phys. Rev.* 137, A1054 (1965).

³⁶C. Cuthbertson and M. Cuthbertson, *Proc. R. Soc. Lond.* 135, 40 (1932); C. R. Mansfield and E. R. Peck, *J. Opt. Soc. Am.* 59, 199 (1969); M. C. E. Huber and G. Tondello, *J. Opt. Soc. Am.* 64, 390 (1974).

³⁷L. R. Ingersoll and D. H. Liebenberg, *J. Opt. Soc. Am.* 46, 538 (1956).

³⁸Many of the techniques employed in determining positions and widths of autostates are cited, for example, by C. A. Nicolaides, *Phys. Rev. A* 6, 2078 (1972).

³⁹The use of an analytically continued Hamiltonian, as discussed, for example, by E. Balslev and J. M. Combes, *Commun. Math. Phys.* 22, 280 (1971), is particularly convenient when only square-integrable basis functions are employed, as in the present development. This approach is pursued in a separate investigation.